JMATPRO

Journal of Advanced Materials and Processing
9 (4): 53-63, Autumn 2021
http://jmatpro.iaun.ac.ir
20.1001.1.2322388.2021.9.4.6.8

Research Paper

GEP-based Modeling for Predicting Sponge Iron Metallization in Persian Direct Reduction (PERED) Method

Mehdi Firouzi[1, 2], Mojtaba Sadeghi[1,3], Mojtaba Firouzi[4], Masoud Kasiri-Asgarani[3*], Hamid Reza Bakhsheshi-Rad[3]

1. Research & Development, Sirjan Jahan Steel Complex (SJSCO), Sirjan, Iran
2. Baft Steel Complex, Baft, Iran
3. Advanced Materials Research Center, Department of Materials Engineering, Najafabad Branch, Islamic Azad University, Najafabad, Iran
4. Department of Computer Engineering, Qom university of Technology, Qom, Iran

ARTICLE INFO

Article history:

Received 25 July 2021
Accepted 2 September 2021
Available online 1 November 2021

Keywords:
PERED
Direct Reduced Iron (DRI)
Gene Expression Programming (GEP)
Mathematical modeling

ABSTRACT

The Persian direct reduction method (PERED) is a suitable method for producing sponge iron on an industrial scale. The challenge of all sponge iron production plants is to supply sponge iron with suitable metallization to steel factories. Accordingly, determining and adjusting the various parameters affecting metallization in each plant is necessary to produce the appropriate amount and quality of sponge iron. In this study, first, the effects of output rate, process flow, water- steam flow rate, bustle temperature, bustle CH_4 level, CO_2 reform, average pellet size (PIDa), pellet strength (CCS), process gas water temperature, and furnace bed average temperature on spongy iron metallization were investigated. Then, an attempt was made to model the sponge iron grade produced by the PERED method using the Gene Expression Programming (GEP) software. To carry out modeling, data on the affecting variables of metallization were collected for 58 days. The best R2 values for the training and testing sets were 0.974 and 0.27 with a low error rate for both (0.047 and 0.376 in RMSE and 0.001 and 0.141 in MSE, respectively. The results of the sensitivity test indicated that CO_2 reform gas, bustle CH_4 level, and average pellet size had the most significant effect on metallization.

Citation: Firouzi, M.; Sadeghi, M.; Firouzi, M.; Kasiri-Asgarani, M.; Bakhsheshi-Rad, H.R., (2021) GEP-based Modeling for Predicting Sponge Iron Metallization in Persian Direct Reduction (PERED) Method, Journal of Advanced Materials and Processing, 9 (4), 53-63. Dor: 20.1001.1.2322388.2021.9.4.6.8

[*] **Corresponding Author**
E-mail Address: m.kasiri.a@gmail.com

1. Introduction

Sponge iron is obtained by directly reducing pellets through which oxygen is removed without melting the iron. With a high grade of iron, this product is highly emphasized nowadays due to its low iron waste, the increase in iron price, and the rising environmental problems [1-6]. After melting the sponge iron in a steel plant, the product is used in the casting process in the form of ingots, billets, slabs, and rebars. The high-grade metallization of sponge iron reduces the cost of the final product in the steelmaking process [7]. However, producing sponge iron at a proper level of metallization to supply to steelmaking plants is the main challenge for the sponge iron production firms. Therefore, identifying and adjusting effective parameters in metallization are necessary for each plant to produce the desired sponge iron [8].

In the literature, numerous direct reduction methods such as HYL, Midrex, etc., have been presented, among which the Persian direct reduction method (PERED) is nowadays receiving significant attention due to better control of influential parameters, e.g., steam [6-7]. In this method, pellets are converted to sponge iron in direct contact with the reduction gas, and the produced gases are reused for obtaining the reduction gas.

In this study, first, the parameters affecting the metallization of sponge iron were identified, which included output rate, process flow, water-steam flow rate, bustle temperature, bustle CH_4 level, CO_2 reform, average pellet size, pellet strength, process gas water temperature, and furnace bed average temperature. Then, data were collected from the Baft Steel Complex Co. on each variable for 58 days. Finally, using Gene Expression Programming (GEP) software, the best model was identified based on the variables, error rate, and regression, and the most effective factor was also determined through a sensitivity test.

2. Process and theoretical background

2.1. Process

The design of four factories adopting PERED® technology (Persian direct reduction method) with the capacity of 800,000 tons of DRI per year was initiated in 2007 and the first PERED® products in the world were produced in 2017 in Iran. A schematic view of PERED® technology is given in Figures 1,2. In this method, the top gas returns from the furnace to the scrubber so that it is cleaned and its temperature is reduced [9]. The reformer burners use one-third of the exhaust gas from the scrubber as an auxiliary fuel, and two-thirds of it is used to produce process gas. The process gas is compressed by compressors and mixed with preheated natural gas. The preheated feed gas enters the reformer, and after transformation into reform gas, it enters the furnace [5]. Mittel et al. introduced the following process for reducing pellets by CO and H_2 [7]:

$$Fe_2O_3+H_2/CO=Fe+H_2O/CO_2 \quad (1)$$

which in turn incorporates the following reactions.

Conversion of hematite to magnetite:

$$Fe_2O_3+H_2/CO=Fe_3O_4+H_2O/CO_2 \quad (2)$$

Conversion of magnetite to wüstite:

$$Fe_3O_4+H_2/CO=FeO+H_2O/CO_2 \quad (3)$$

Conversion of wüstite to iron:

$$FeO+H_2/CO=Fe+H_2O/CO_2 \quad (4)$$

Reform reactions are heating ones. The heat for the CH_4 reform reaction is provided by natural gas and fuel in the reformer box [10]. Atsushi et al. introduced the following reactions within the reformer [11].

$$CH_4+ H_2O \rightarrow CO +3H_2 \quad (5)$$

$$CH_4 +CO_2 \rightarrow 2CO +2H_2 \quad (6)$$

$$2CH_4 + O2 \rightarrow 2CO + 4H_2 \quad (7)$$

$$CO +H_2O \rightarrow CO_2 + H_2 \quad (8)$$

$$CH_4 \rightarrow C(s) + 2H_2 \quad (9)$$

$$CO + C \rightarrow CO_2 \quad (10)$$

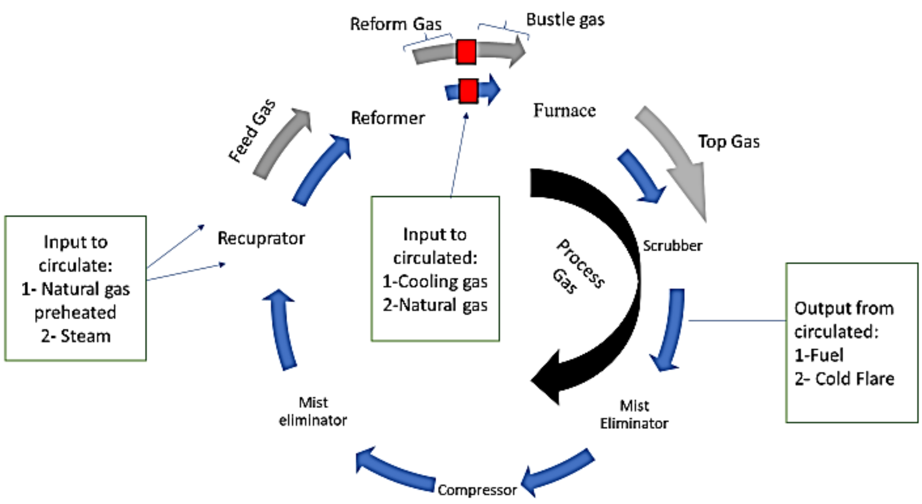

Fig. 1. Schematics of the process gas circle

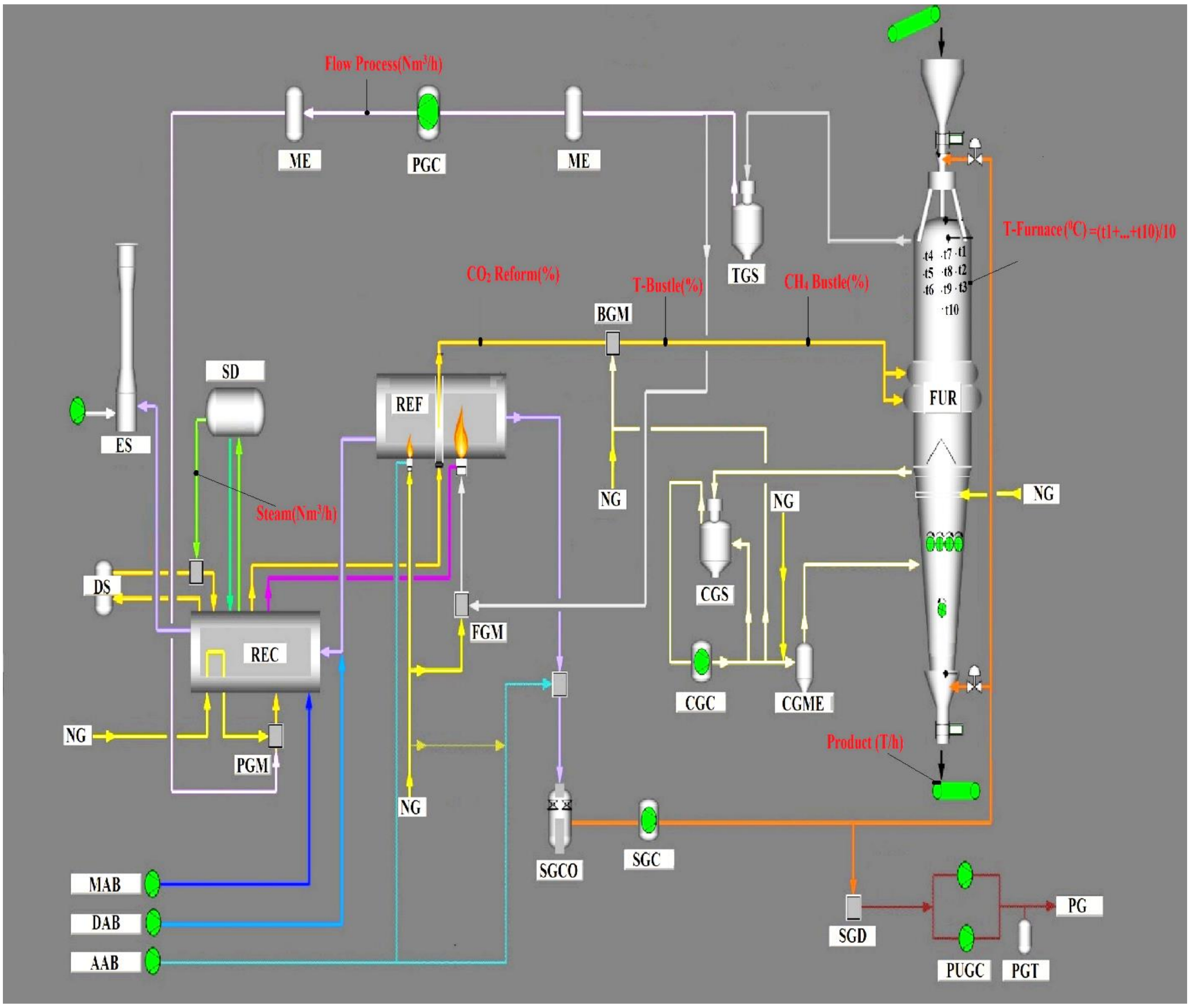

Fig. 2. Schematics of PERED sponge revitalization process

Table 1. Acronyms and abbreviations for the equipment in Fig. 1

Abbreviation	Full name
TGS	Top gas scrubber
ME	Mist eliminator
PGC	Purge gas compressor
SD	Steam drum
ES	Ejector stack
DS	Desulfurization
REC	Recuperator
PGM	Process gas mixer
NG	Natural gas
MAB	Main air blower
AAB	Auxiliary air blower
DAB	Dilution air blower
REF	Reformer
FGM	Fuel gas mixer
BGM	Bustle gas mixer
SGCO	Seal gas compressor
SGC	Seal gas cooler
SGD	Seal gas dryer
PUGC	Purge gas compressor
PT	Purge gas tank
PG	Purge gas
CGS	Cooling gas scrubber
CGC	Cooling gas cooler
CGME	Cooling gas mist eliminator
CGCO	Cooling gas cooler
FUR	Furnace

2.2. Gene Expression Programming (GEP)

The GEP technique has been inspired by the process of translating information into proteins in biological genes encoded in DNA. GEP algorithms are employed to determine the best relationship between input and output variables using a primary accidental population of chromosomes, suitability function (as a measure of accuracy), and mathematical and genetic operators [12]. The main elements of GEP are chromosomes and Expression Trees (ETs). A chromosome is made up of one or more genes represented by a mathematical equation [13]. Each gene has two components, namely a head and a tail. The head of a gene, comprising mathematical operators, variables, and constants, is used to encode a function. Its tail, on the other hand, consists only of variables. The constants are used as complementary terminal symbols [14].

The main solutions to a problem are first encrypted by chromosomes and subsequently translated into ETs. Valid ETs and each specific gene are generated using continuous genetic mutation as a result of translating chromosomes into ETs. Fig. 3 shows the translation of a chromosome with two genes into an ET and its corresponding mathematical equation.

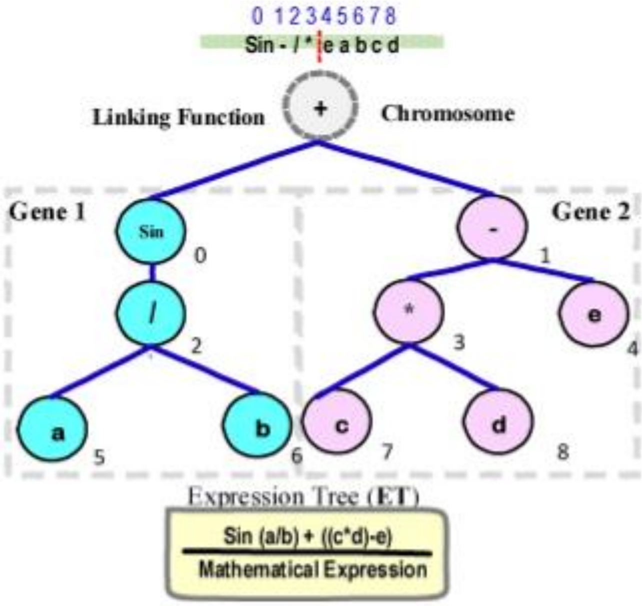

Fig. 3. Translation of a chromosome with two genes into an ET and its corresponding mathematical equation

Further research on GEP operational guidelines can be found in the literature. In this study, chromosomes are randomly generated from the primary population. The chromosomes' expression is completed in the next step, and each chromosome's cost is calculated based on the selected performance. Chromosomes are multiplied or modified according to the chosen cost or error value. This process is repeated until the desired number of generations or the appropriate model error is obtained [15].

In general, in the first stage of the GEP flowchart, the initial population, which is coded and not executable, is created randomly. Then, the flowchart should be introduced and expressed, and afterward, the program that lies in the gene will be executed and used to achieve the output value. A fitness function is evaluated for each chromosome, and if the number of program runs is not met, the next generation is processed. The best chromosomes are transferred to the next generation without any mutation through pure elitism. Then, the process of replication and reproduction is carried out similarly to that in nature, but faster now for genetic operators. The selection chromosomes are made up of the chromosomes in the previous generation. The process is repeated until a proper fit is achieved or the limitation for the number of repetitions of the program is met. The process of replication and reproduction of chromosomes is executed at the rates set by the designer [16]. The performance of the GEP models was .evaluated through the following statistical quality criteria: coefficient of determination (R2), Mean Absolute Error (MAE), Mean Square Error (MSE), and Relative Root Square Error (RRSE). The RMSE and RRSE equations are given below. In these equations, n is the number of data, ya represents the experimental value, and yp stands for the predicted value. The RRSE was more consistent than the RMSE in most cases.

$$R^2 = 1 - \frac{\sum_{i=1}^{n}(y_a - y_p)^2}{\sum_{i=1}^{n}(y_a - \bar{y}_a)^2}, MSE = \frac{1}{n}\sum_i (ya - yp)^2, RMSE = \sqrt{\frac{1}{N}\sum_1^N \left(y_p - y_a\right)^2},$$

$$RRSE = \sqrt{\frac{\sum_i (ya - yp)^2}{\sum_i \left(ya - \left(\frac{1}{n}\right)\sum_i ya\right)^2}} \quad (11)$$

3. Methodology and MD percentage prediction of sponge

The main variables that affect the grade of sponge iron are output rate, process flow, water-steam flow rate, bustle temperature, bustle CH_4 level, CO_2 reform, average pellet size, pellet strength, process gas water temperature, and furnace bed average temperature. The following equation can express metallization:

MD=F(CCS, average pellet size (PIDa), T-Bustle, T-average furnace, Steam, flow/ton, CH_4 bustle, CO_2 reform)

Since the rate of change in the injected CH_4 to the transition area and the China hat are constant and the percentage of oxygen in the low sealing gas is low, these variables were not considered in modeling by the GEP software. Table 2 shows the input values of eight variables collected in 58 days from the Baft Steel Complex Co. as well as metallization per day (output).

The data were divided into two different groups, with 80% for training and the rest for testing. Twelve samples per day (one sample every two hours) were taken from the furnace output, and metallization was determined by the titration method in the laboratory. In the table, the mean of all the 12 metallization values for each day is given to reduce the error. The strength and size of 30 pellets were measured using a strength meter, and their average values were determined. Other variables were reported in daily average values read from analyzers and thermocouples installed on the lines and the furnace substrate. To reduce the error, the average changes of parameters per day were used. The data for 58 days from March to May are reported in Table 2.

Table 2. Input values of eight variables collected in 58 days from the Baft Steel Complex Co.

CCS (Ave) (kg/P)	PIDa (Ave) (mm)	Flow/ton ((Nm3/h)/(T/h))	CO_2 reformed (%)	Bustle CH_4 (%)	Bustle temp. (°C)	Average furnace temp. (°C)	Steam (Nm^3/h)	Metalization (%)
258	10.95	950	2.49	4.59	827	743	10155	92.25
231	11.59	946.215	2.5	4.51	824	742	10202	92.1
250	11.9	960.486	2.35	4.45	826	741	10191	90.85
229	11.48	983.573	2.41	4.54	826	746	10198	91.89
235	11.69	964.228	2.51	4.43	826	753	10125	92.31
265	12.32	963.623	2.62	4.44	824	755	10213	92.31
245	11.79	954.724	2.63	4.4	824	751	10213	92.18
238	11.63	951.772	2.64	4.45	824	746	10305	91.46
241	11.83	989.44	2.55	4.52	824	748	10102	91.07
244	11.19	962.222	2.74	4.6	827	746	10227	91.39
252	11.43	957.453	2.75	4.55	826	743	10242	91.00
252	11.57	960.241	2.68	4.48	824	742	10247	91.10
253	11.99	972.467	2.72	4.46	825	741	10239	91.52
240	12.07	990.895	2.5	4.49	824	744	10491	91.62
282	12.02	969.48	2.69	4.44	825	747	10268	91.91
263	11.79	950.98	2.76	4.46	825	748	10065	91.31

265	11.73	954.58	2.69	4.56	825	749	10331	91.19
229	11.59	960.667	2.55	4.48	826	755	10805	92.26
268	10.91	960.366	2.64	4.47	825	751	10720	91.30
225	11.88	960.934	2.54	4.54	825	750	10926	92.24
226	11.67	950.98	2.63	4.56	825	749	10298	91.88
237	11.78	951.02	2.7	4.6	825	755	10749	92.6
219	11.91	950.98	2.65	4.5	825	754	10360	92.59
231	11.82	950.98	2.62	4.48	825	753	10444	92.59
226	11.64	950.941	2.65	4.53	825	752	10532	92.76
213	12.08	951.01	2.73	4.47	825	747	10568	92.44
246	12.01	934.127	2.62	4.43	827	740	10481	92.64
235	11.57	954.685	2.6	4.57	825	762	10542	92.35
261	11.46	932.303	2.28	4.44	825	755	10495	92.69
252	11.44	925.392	2.42	4.34	826	749	10532	92.47
234	11.93	950.941	2.59	4.31	825	748	10529	91.71
242	11.59	950.11	2.57	4.31	826	757	10396	91.34
242	11.28	930.23	2.37	4.3	826	757	10579	92.25
207	12.2	950.455	2.42	4.32	825	749	10543	92.92
205	11.45	947.442	2.35	4.54	825	752	10579	92.78
275	11.46	947.4	2.46	4.48	827	758	10357	92.6
235	11.24	947.347	2.4	4.56	825	752	10297	92.76
250	11.75	947.126	2.37	4.44	825	753	10200	92.6
261	11.67	944.642	2.35	4.42	824	745	10190	93.02
257	11.51	940.418	2.36	4.38	825	737	10237	92.57
276	11.52	937.267	2.58	4.46	825	744	9821	93.25
264	11.66	927.845	2.63	4.54	827	743	9674	92.39
236	12.06	927.784	2.63	4.5	825	744	9630	91.56
256	11.68	933.6	2.6	4.49	825	741	9801	92.31
257	11.66	925.063	2.57	4.44	825	744	9615	92.41
223	11.89	937.458	2.63	4.5	825	747	9956	92.7
247	12.34	941.369	2.63	4.59	825	748	9711	92.25
295	11.68	937.49	2.62	4.54	825	743	9804	92.42
248	12.02	931.083	2.54	4.49	824	742	9909	92.04
281	11.57	937.49	2.56	4.48	825	748	9861	92
255	11.55	937.51	2.58	4.55	827	748	9955	91.72
266	11.61	937.51	2.56	4.55	827	747	9736	91.79
256	11.68	936.604	2.57	4.49	825	748	10107	91.65
282	12.13	947.337	2.53	4.44	825	763	10034	92.39
279	11.78	947.4	2.59	4.44	825	756	9876	93.28
262	12.67	932.53	2.62	4.46	825	757	9873	92.73
231	12.06	975.969	2.84	4.68	827	753	9667	93.32

Percentage of spongy iron metallization was estimated using GeneXpro Tools 5.0 software on an Intel®core (TM) i5-4200U, 1.6GHz, personal computer. To evaluate the accuracy of the proposed model, Root Mean Square Error (RMSE) and Relative Root Square Error (RRSE) were adopted as fitness functions. Then, the chromosomes were produced from terminal sets, the basic arithmetic operators {+, ×, −, /}, and other mathematical functions, e.g. log, exp, power, tanh, cubic root, etc. The effective parameters in GEP software were selected such that the best model was obtained with the lowest complexity. To this end, the number of optimal genes and chromosome heads was determined and additional or multiplication operators were used as interconnection functions between ETs. Finally, a combination of genetic operators including mutation, inversion, transfer, and recombination was selected. The GEP parameters changed in each run, and the training and test performances were monitored for each model. Table 3 summarizes these parameters. They were selected through trial and error to obtain the desired results. Output rate, process flow, water-steam flow rate, bustle temperature, bustle CH_4 level, CO_2 reform, average pellet size, pellet strength, process gas water temperature, and furnace bed average temperature were accounted for as the input layers. Table 4 shows the parameters of the GEP models with a regression power above 96%. The number of functions varied between 7 and 10 and in all models, the main mathematical operators ("+", "-", "and," and "/") were included. Other functions were also employed when needed ("3Rt," "Sqrt," "Sin," "exp," "tanh," "Atan," "Asech," "x2," "x3," "x4," and " log ").

4. Pre-processing of collected data

Using box plots, the out-of-range data were identified and removed (Figure 4). As a result, eight data were disregarded, and the number of data reached 49 (Table 3). The control room operator tried to keep the variables in the proper range by controlling the temperature of the reformer, the injected gas, and other parameters.

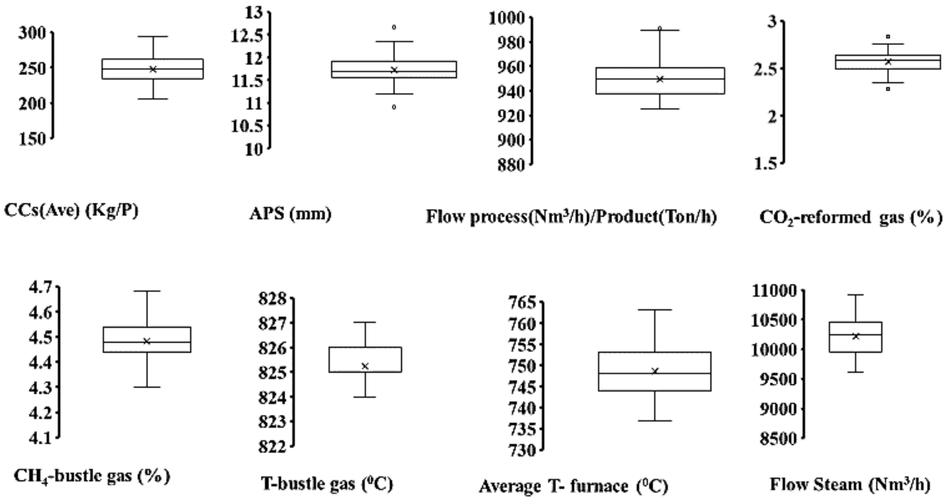

Fig. 4. Box plots for determining the out-of-range data

Table 3. The obtained 49 data after omitting the out-of-range data

CCS (Ave) (kg/P)	PIDa (Ave) (mm)	Flow/ton ((Nm^3/h)/(T/h))	CO_2 reformed (%)	Bustle CH_4 (%)	Bustle temp. (°C)	Average furnace temp. (°C)	Steam (Nm^3/h)	Metalization (%)
231	11.59	946.215	2.5	4.51	824	742	10202	92.1
250	11.9	960.486	2.35	4.45	826	741	10191	90.85
235	11.69	964.228	2.51	4.43	826	753	10125	92.31
265	12.32	963.623	2.62	4.44	824	755	10213	92.31
245	11.79	954.724	2.63	4.4	824	751	10213	92.18
238	11.63	951.772	2.64	4.45	824	746	10305	91.46
244	11.19	962.222	2.74	4.6	827	746	10227	91.39
252	11.43	957.453	2.75	4.55	826	743	10242	91.00
252	11.57	960.241	2.68	4.48	824	742	10247	91.10
253	11.99	972.467	2.72	4.46	825	741	10239	91.52
282	12.02	969.48	2.69	4.44	825	747	10268	91.91
263	11.79	950.98	2.76	4.46	825	748	10065	91.31
265	11.73	954.58	2.69	4.56	825	749	10331	91.19
229	11.59	960.667	2.55	4.48	826	755	10805	92.26
225	11.88	960.934	2.54	4.54	825	750	10926	92.24
226	11.67	950.98	2.63	4.56	825	749	10298	91.88
237	11.78	951.02	2.7	4.6	825	755	10749	92.6

219	11.91	950.98	2.65	4.5	825	754	10360	92.59
231	11.82	950.98	2.62	4.48	825	753	10444	92.59
226	11.64	950.941	2.65	4.53	825	752	10532	92.76
213	12.08	951.01	2.73	4.47	825	747	10568	92.44
246	12.01	934.127	2.62	4.43	827	740	10481	92.64
235	11.57	954.685	2.6	4.57	825	762	10542	92.35
252	11.44	925.392	2.42	4.34	826	749	10532	92.47
234	11.93	950.941	2.59	4.31	825	748	10529	91.71
242	11.59	950.11	2.57	4.31	826	757	10396	91.34
242	11.28	930.23	2.37	4.3	826	757	10579	92.25
207	12.2	950.455	2.42	4.32	825	749	10543	92.92
205	11.45	947.442	2.35	4.54	825	752	10579	92.78
275	11.46	947.4	2.46	4.48	827	758	10357	92.6
235	11.24	947.347	2.4	4.56	825	752	10297	92.76
250	11.75	947.126	2.37	4.44	825	753	10200	92.6
261	11.67	944.642	2.35	4.42	824	745	10190	93.02
257	11.51	940.418	2.36	4.38	825	737	10237	92.57
276	11.52	937.267	2.58	4.46	825	744	9821	93.25
264	11.66	927.845	2.63	4.54	827	743	9674	92.39
236	12.06	927.784	2.63	4.5	825	744	9630	91.56
256	11.68	933.6	2.6	4.49	825	741	9801	92.31
257	11.66	925.063	2.57	4.44	825	744	9615	92.41
223	11.89	937.458	2.63	4.5	825	747	9956	92.7
247	12.34	941.369	2.63	4.59	825	748	9711	92.25
295	11.68	937.49	2.62	4.54	825	743	9804	92.42
248	12.02	931.083	2.54	4.49	824	742	9909	92.04
281	11.57	937.49	2.56	4.48	825	748	9861	92
255	11.55	937.51	2.58	4.55	827	748	9955	91.72
266	11.61	937.51	2.56	4.55	827	747	9736	91.79
256	11.68	936.604	2.57	4.49	825	748	10107	91.65
282	12.13	947.337	2.53	4.44	825	763	10034	92.39
279	11.78	947.4	2.59	4.44	825	756	9876	93.28

5. Results and discussion

All of the models have values higher than 0.87 (table 4), indicating their suitability for predicting the percentage of iron metallization. GEP-1 model has the highest R2 among all the selected GEP models. The proposed model equations for GEP-1 to GEP-8 are summarized in Table 4. The models were extracted from their corresponding ETs. The large size of some equations indicates the complex space between the applied parameters.

Table 4. The proposed model equations for GEP-1 to GEP-8

Model	Acquired equation
GEP-1	$-1.59d_6 +d_4+d_3+d_5+ (d_6+(((((-5.6-d_0)(d_0-d_1))(-5.6-(d_0-d_6)))-d_3)-d_4)) + (1.11d_3(((((1.11d_4+1.23)(d_1d_2d_4))-d_6)) +0.83d_1-0.095 + (0.634((((d_3d_6d_6))-2d_3)-((d_7/0.634)0.634))d_3))+ (0.507+d_4) + (-0.494-(-0.494((((d_2+0.494)(d_4-d_7))(d_4+d_1))(-0.494+(-0.494d_0)))))+ (d_3-d_5)+ ((((d_7+d_7)(-0.149d_1))-d_2)-((-0.149+(d_6-0.149))((-0.149-d_2)+1)))+ ((0.138-d_4)0.138) + (d_4d_1)(((d_3-d_4)+((d_0-0.84)(-0.84)))d_4))$
GEP-2	$(0.24d_7) + (d_7(d_4-((((d_1-d_5)+0.108)+0.108)((d_2-d_0)d_7)))) + (d_7+(((1.54(0.779-d_7)d_2))+(d_2d_0d_1)))+ (((d_3^2)(((d_0^2)-d_7)^2))+(d_7-d_2))))+ ((((d_2-d_0)^2)-(0.62d_3))((0.62d_3)+d_0))+0.45$
GEP-3	$((d_2-d_7)((d_7(((d_1d_1)-d_3)/0.34))-d_4)) + ((((d_2-d_5)-0.39)0.39)^2)+ (0.53d_0)+ ((0.179d_7)d_7) + (((((d_6-d_1)(d_1+d_1))+((d_3-d_0)-d_4))((-0.51d_4)+(-0.51d_4)))d_4) + (d_4-(d_1-d_7)) + ((((d_2-(-0.51+d_0))(d_2+d_1))-(d_6+(d_2^2)))+(d_1^2)) + (d_6+((1.0-(((0.71+d_0)(0.84d_7)+0.84))-(d_7^2))) + (((d_0+(2.1+d_1))-(d_1+d_0))+(((1-d_3)-2.1)-(1-d_0)))$
GEP-4	$((((1.0-d_7)(1.0+0.61))((d_7-0.61)+(d_1+d_4)))((0.3721)) + (((0.25d_3((((d_4-0.25)d_5)+d_4)))-0.25)-d_3)+ ((d_0)(\mathrm{sqrt}d_0+(1.0-(d_2-(d_2d_3))))) + ((-0.177-d_3)+0.177+ ((d_2(0.64d_6))+(d_3+(0.72-d_2)))+ (d_6+((1-((1+(d_6/0.99))-0.99))-((d_7+(-0.99d_7)d_7))) + (((d_2+(d_2-d_3))-((d_7d_7)(d_3-d_4)))(d_2((1.0-2.82)-(d_0+d_4)))) + (\mathrm{sqrt}(d_6)-d_4) + ((0.36d_6)-d_6^2)+ ((((((d_3d_2)-d_6)-d_0)+((d_7+d_6)d_4))-0.44)-0.44) + ((d_6d_3d_3(d_6-d_3))))(((d_3+5.26)+(d_0+d_3))-d_5))$
GEP-5	$\mathrm{pow}(\mathrm{pow}(((((d_3d_3)+(d_2-d_0))((d_6d_3)(d_0+d_4)))-((0.18+d_3)\mathrm{pow}(d_0,2))),2),2)+ (1-\exp(d_1))+(d_5d_6d_1-(d_2-d_4))))+(d_1*((((d_1-d_7)(d_2d_3))+0.23+(\mathrm{pow}(d_1,2)d_7)))+0.29+ (d_1(1-((((d_7-d_1)+\mathrm{pow}(d_6,2))\mathrm{pow}((d_3/0.6),2))((d_3d_6)(d_0-d_1)))))+ (\exp((d_0-((d_1d_0)+0.6)))((0.6-(d_3d_3))-(d_0d_7d_5)))$
GEP-6	$(1-d_4) + (d_5(2d_7+d_3-1.48)-\tan(d_6-d_0)^5-d_5) + \tan d_0^3 + 0.207d_7^3d_7+d_6d_1^3-d_0-0.52+ (1-d_5)^5-2.79(1-d_4)(d_3d_5^2) +((-0.092-d_2+\tan d_7)(\tan d_4+0.62)-\tan(d_7+0.62-d_5)-0.51((d_1+d_2)-(d_7-d_4)))^3)(d_0d_2+0.51))/(1.51-d_4 + d_4-(4.98(d_3+d_2^3+9.96)-4.98))+d_2)$
GEP-7	$((((d_2-d_1)((d_6-d_7)-d_2^{1/3}))-d_1))^{1/3}(\mathrm{atan}((((d_4-0.37)+d_4)-0.123))((0.37-d_0))d_1)^{1/3}+ (1.0-d_2)+ (((((d_5d_7)-0.67)^2))^2)^{1/3}(d_0-\mathrm{atan}(d_4))) \quad \mathrm{atan}d_6 \ (-1+d_2 + \mathrm{atan}((1-((((-1.7d_2)+1.7)^2)(-1.7d_4))))$
GEP-8	$(-0.392-(((\mathrm{sqrt}(d_6)(d_0d_4))(-0.39d_6))((d_7+0.392)-0.392-d_7)))(1.0-(d_0+((((-0.68-d_0)(d_0-0.34))(d_0-(d_0d_7)))))\ ((((d_7^2-(-3.98d_7))-3.98-d_0)(d_2-d_2^2))d_3)\ (\mathrm{atan}((1-d_2))-0.1681d_7/(0.41+d_7))+d_6)))(d_6\sin((((0.41(d_0+d_6))-((d_6*d_4)-d_7))^2)))$

Table 5. Variables in Table 4

Variable	Symbol
Pellet strength (CCS)(kg/P)	d_0
Average pellet size (PIDa)(mm)	d_1
Flow process (Nm^3/h)/product (T/h)	d_2
CO_2 reform (%)	d_3
Bustle CH_4 (%)	d_4
Bustle temperature (°C)	d_5
Average temperature of furnace (°C)	d_6
Steam (Nm^3/h)	d_7

As shown in Tables 6 and 7, the numbers of genes and mathematical functions as well as their linking function and types have a significant effect on the performance of a GEP model. For example, at the same speed as that of the genetic operator, GEP-1 (R2train = 0.974) and GEP-7 (R2train = 0.874) models with the mathematical function of 10 have the highest and lowest training performances among the developed models. Sensitivity analysis was carried out to determine the effect of the applied parameters on the percentage of sponge iron. Since GEP-1 was the best model for predicting the percentage of spongy iron metallization, it was chosen for the analysis. Fig. 5 shows the results of sensitivity analysis for the input variables of metallization.

Table 6. Random changes of GEP software setting

Model	Linking function	Head size	Number of genes	Number of functions	Type of function
GEP-1	Addition	13	13	10	+, −, ×, /
GEP-2	Addition	12	6	10	+, −, ×, /, x^2
GEP-3	Addition	12	9	10	+, −, ×, /,SqrtX,X^2, complement ,LnX,
GEP-4	Addition	13	11	10	+, −, ×, /,X^2,complement
GEP-5	Addition	13	7	10	+, −, ×, / ,X^2
GEP-6	Addition	13	8	10	+, −, ×, /,complement, log(x,y),sqrt(x),X^3,X^5,Tan(X)
GEP-7	Multiplication	10	7	10	+, −, ×, /,complement, log(x,y),sqrt(x),$X^{1/3}$,X^2,Tan(X),arctan(X)
GEP-8	Multiplication	11	5	10	+, −, ×, /,complement, log(x,y),sqrt(x),X^2,arctan(X)

Table 7. Errors and regressions of the training and test data

No.	R^2		Training			Testing		
	Training	*Testing*	*RMSE*	*MSE*	*RRSE*	*RMSE*	*MSE*	*RRSE*
GEP-1	0.974	0.273	0.041	0.001	0.158	0.376	0.141	1.644
GEP-2	0.932	0.103	0.068	0.004	0.260	0.362	0.131	1.200
GEP-3	0.924	0.108	0.081	0.006	0.279	0.557	0.310	1.365
GEP-4	0.884	7.01	0.089	0.007	0.342	0.301	0.090	1.356
GEP-5	0.921	0.285	0.071	0.005	0.282	0.325	0.106	1.070
GEP-6	0.883	7.86	0.098	0.008	0.342	0.773	0.597	3.55
GEP-7	0.874	3.722	0.096	0.009	0.360	0.392	0.153	1.957
GEP-8	0.911	0.288	0.081	0.006	0.298	0.435	0.189	1.314

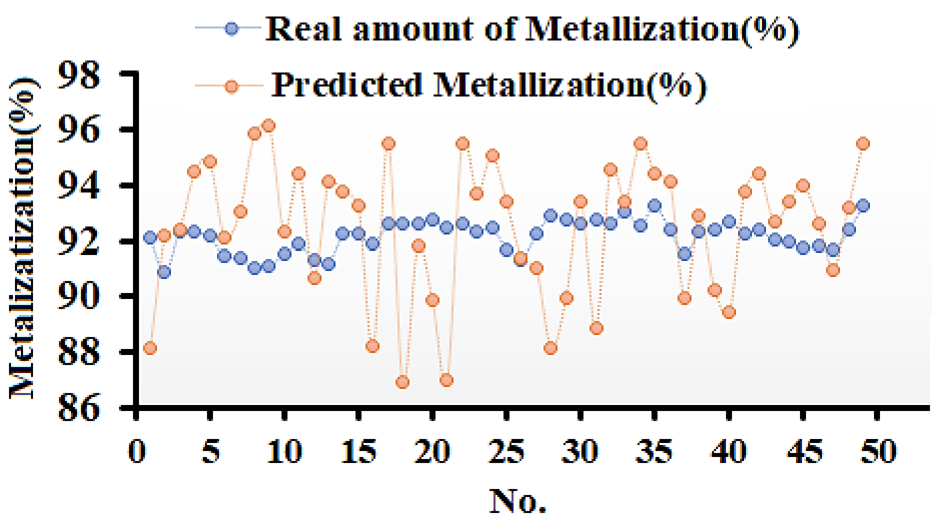

Fig. 5. Real and predicted percentage of metallization with residual values acquired for the GEP-1 model

The percentage of CO_2 gas reform, bustle CH_4 level, and average pellet size are the most influential parameters, while other variables exert negligible effects on the model's predictive performance. In general, the CO_2 gas reform percentage shows the CO_2 amount that has not entered the reaction through the CH_4 reform tubes. Increased CO_2 reform indicates the rise in the amount of H_2O(g) in the system and methane gas failure entry into the reaction with water steam due to the lower enthalpy of their reaction. Moreover, in this situation, the percentage of revitalized H_2 gas is more than that of CO. Hence, revitalization reactions in the furnace occur more with H_2 than with CO, and since H_2 is smaller in size, the penetration of the revitalization gas at the constant retention time of pellet in the furnace is higher. As a result, metallization is improved. This is true as long as the increase in CO_2 reform is within the appropriate range of 2.3 to 3%. CO_2 reform amounts higher than the mentioned range lead to a decrease in the furnace bed temperature due to endothermic reactions in the furnace, including the Boudouard reaction.

An increase in bustle CH_4 percentage with the occurrence of the in-pace reform reactions (methane failure reactions on the porous surface of sponge iron and pellet as a catalyst) enhances the production of the revitalization gas and, consequently, metallization. However, beyond the proper range of 3.2 to 4.5, because of the occurrence of in-place endothermic reform reactions, the furnace bed temperature decreases. One of the other effective parameters is average pellet size (PIDa). With bigger pellets at a constant retention time in the furnace, there is little opportunity for revitalization of the center of the pellet, hence a decrease in metallization.

6. Conclusion

1- Gene Expression Programming (GEP) was proposed to predict the metallization percentage of sponge iron through PERED.

2- The parameters affecting the leached percentage of metallization were output rate, process flow, water-steam flow rate, bustle temperature, bustle CH_4 level, CO_2 reform, pellet granulation, and pellet strength.

3- The best R2 values for the training and testing sets were 0.974 and 0.27 with a low error rate for both (0.047 and 0.376 in RMSE and 0.001 and 0.141 in MSE, respectively). Also, sensitivity analysis of metallization parameters showed that the percentage of CO_2 gas reform, bustle CH_4 level, and pellet granulation were the most influential parameters in the metallization percentage of sponge iron. The proposed technique can be employed in predicting the optimum elements in the operational PERED process.

References

[1] S. Baig, B. Murray: Duke Univ., 2016.
[2] F.M. Mohsenzadeh, H. Payab, M.A. Abdoli, Z. Abedi, Ekoloji, 27(2018) 959–967.
[3] M. Kazemi, M. Saffari pour, D. Sichen: Metallurgical and Materials Transactions B., 2017, vol. 48B, pp. 1114–1122.
[4] G. KIM, P. C. Pistorius: Metallurgical and Materials Transactions B., 2009, vol. 40B, pp. 17–24.
[5] E. A. Mousa, A. Babich, D. Senk: Metallurgical and Materials Transactions B., 2013, vol. 45, pp. 617–628.
[6] I. Sohn, R. J. Fruehan: Metallurgical and Materials Transactions B., 2013, vol. 36B, pp. 605–612.
[7] F. M. Mohsenzadeh, H. Payab, M. A. Abdoli, Z. Abedi: Ekoloji., 2017, Vol. 27, pp. 959–967.
[8] P. Cavaliere: Ironmaking and Steelmaking Pro., 2019, pp. 419–484.
[9] B. Voelker, H. Michishita, T. Wright: Google Patents., 2020.
[10] B. Anameric, S. K. Kawatra: Miner. Process. Extr. Metall. Rev., 2007, vol. 207, pp. 59–116.
[11] F. O. Boechat, R. M. de Carvalho, L. M. Tavares: KONA Powder Part., 2018, Vol. 35, pp. 216–225.
[12] M. Khosravi, M. Zeraati: Particle Science and Tech., 2019, Vol. 5, pp. 145-159
[13] A. D. Mehr: Hydrol., 2018, Vol. 563, pp. 669–678.
[14] H. Ebrahimzade, G. R. Khayati, M. Schaffie: Environ. Chem. Eng., 2018, Vol. 6, pp. 3999–4007.
[15] L. ZHANG, T. Qiu-hua, C. A. Floudas, D. Ming-xing,: Mach. Des. Manuf., 2017, Vol. 2, pp. 51-60.
[16] A. K. Sista Kameshwar, W. Qin: Mycology., 2020, Vol. 11, pp. 22-37.